Design, Synthesis, and Multivariate Quantitative Structure−Activity Relationship of Salicylanilides—Potent Inhibitors of Type III Secretion in *Yersinia*

Markus K. Dahlgren, Anna M. Kauppi, Ing-Marie Olsson,† Anna Linusson, and Mikael Elofsson*

Department of Chemistry, Umeå University, SE-901 87 Umeå, Sweden

Received June 24, 2007

Analogues to the salicylanilide *N*-(4-Chlorophenyl)-2-acetoxy-3,5-diiodobenzamide, **1a**, an inhibitor of type III secretion (T3S) in *Yersinia*, were selected, synthesized, and biologically evaluated in three cycles. First, a set of analogues with variations in the salicylic acid ring moiety was synthesized to probe possible structural variation. A basic structure−activity relationship was established and then used to cherry-pick compounds from a principal component analysis score plot of salicylanilides to generate a second set. A third set with increased likelihood of biological activity was designed using D-optimal onion design. A quantitative structure−activity relationship model using hierarchical partial least-square regression to latent structures (Hi-PLS) was computed using PLS score vectors of building blocks correlated to the % inhibition of T3S as a response. A PLS discriminant analysis (PLS-DA) model was derived using the same descriptor set as that for the Hi-PLS model. Both models were validated with an external test set.

1. Introduction

Excessive use of antibiotics is generally accepted to be the main reason for increased antibiotic resistance among bacteria.[1,2] The spread of resistance is hard to control since it proliferates through gene transfer.[3] Although more restrictive use of antibiotics has a buffering effect, additional approaches to microbe control are needed.[4] Most research so far has been focused on Gram-positive bacteria due to the fact that the most serious cases of resistance have, thus far, occurred in Gram-positives.[5] It is, most likely, only a matter of time before the resistant Gram-negative strains become an equally serious threat. A century ago, tuberculosis, pneumonia, and diarrhea were feared as they were lethal diseases. We are steadily approaching that same situation today. Stomach disorders caused by *Yersinia* spp., *Salmonella* spp., and *Shigella* spp. cause 18% of the bereavements among children under 5 years in developing countries, according to the world health organization (WHO[a]) World Health Report 2005. Today, plague is a controlled disease, but infections and deaths are still reported, and resistant strains have been found.[4] Additionally, one cannot overlook the risk of multiresistant *Y. pestis* being used as a bioterrorism weapon.[6,7] Multiresistant bacteria might be the biggest threat to global health according to WHO. Thus, it is of utmost importance to develop new efficient antibacterial agents attacking bacterial functions, not yet targeted by human efforts in both Gram-positive and Gram-negative bacteria.[8−10]

The type III secretion (T3S) system of *Yersinia* is a virulence system which is shared by many different bacteria, including *Salmonella* spp., *Pseudomonas aeruginosa*, *Chlamydia* spp., *Shigella* spp., and enteropathogenic *Escherichia coli*, which all require T3S for virulence.[11] *Y. pestis*, the agent of Black Death, *Y. pseudotuberculosis*, which causes adenitis and septicaemia, and *Y. enterocolitica*, which inflicts a broad range of gastrointestinal syndromes, are all members of the *Yersinia* genus and are pathogenic to man.[12,13] Research has revealed the major molecular events during *Yersinia* infection,[11,14−16] and *Yersinia* thus serves as an excellent model to study T3S and identify inhibitors[16,17] of the plasmid-encoded Ysc (*Yersinia* secretion) T3S system. In contact with a eukaryotic cell, a number of Yop *Yersinia* outer proteins (Yops) and specific Yop chaperones are expressed. The chaperones protect the Yops on their way to the Ysc apparatus, which is a membrane-associated complex of some 20 proteins that span the inner and outer membrane of the bacterium. At the Ysc apparatus, a number of accessory proteins assist the translocation of the Yops to the cytosolic lumen of the eukaryotic cell via a pore in the membrane that is formed by certain *Yersinia* proteins. The effector proteins (YopE, YopH, YpkA, YopJ, YopM, and YopT) all target specific functions of the eukaryotic cell, including phagocytosis and inflammatory responses.[14]

The translocation of the Yops is essential to evade the host's immune defense, and it is of interest to design and synthesize molecules that can inhibit the secretion or its regulation. This could result in an antibacterial response without killing the bacteria, which hopefully will hinder bacteria from developing resistance but will also have an effect on bacteria that already have developed resistance against conventional antibiotics. Since the T3S systems are highly conserved among Gram-negative bacteria, it is likely that compounds targeting the T3S machinery in *Yersinia* also may affect the T3S machinery in other species, as has been shown for salicylidenacylhydrazides that target T3S in both *Yersinia* and *Chlamydia*.[18−22] Up to date, a number of studies regarding virulence inhibitors and T3S as a potential target have been presented. Most studies involve salicylidenacylhydrazides,[19−23] but additional structures have been reported.[19,24,25] In addition to these inhibitors that target the actual T3S machinery or its regulation, screening-based approaches have also been used to identify inhibitors of specific effector proteins that are delivered into host cells by T3S.[26,27] The strategy to target virulence is attractive,[8,28,29] and a recent study

* To whom correspondence should be addressed. E-mail: mikael.elofsson@chem.umu.se. Telephone: +46-90-7869328. Fax: +46-90-138885.

† Current address: Umetrics AB, Stortorget 21 SE-2113, Malmö, Sweden.

[a] Abbreviations: PLS, partial least-square regression to latent structures; Hi-PLS, hierarchical PLS; T3S, type III secretion; PCA, principal component analysis; DOOD, D-optimal onion design; WHO, world health organization; Yops, *Yersinia* outer proteins; Ysc, *Yersinia* secretion; SAR, structure−activity relationship; QSAR, quantitative structure−activity relationship; BB, building block; SMD, statistical molecular design; PLS-DA, PLS discriminant analysis; ETEC, Enterotoxigenic *Escherichia coli*; TCS, two-component system; YPIII, *Yersinia pseudotuberculosis* serotype III; BHI, brain heart infusion.

10.1021/jm070741b CCC: $37.00
Published on Web 11/02/2007

indicates the strong capacity of bacteria to overcome the effect of inhibitors that target metabolic functions.[30]

A general method used today within the pharmaceutical industry and academia to find starting points for drug development is to screen large collections of compounds in various assays.[31] It is possible to identify small-molecule virulence inhibitors in the absence of target structural information by using high-throughput whole-cell phenotypic assays.[32] These large-scale screens are generally termed high-throughput screening. Hits from the screening are further evaluated to verify that the identified response is not due to side effects (false positives). A basic structure−activity relationship (SAR) is usually established to ensure that the structure can be varied and still retain biological activity. To find more biologically active compounds, various computational methods are frequently utilized.[33] If a protein structure is known, molecular docking of virtual libraries into the binding site of the target protein can be done. Another useful method is statistical molecular design[34−36] (SMD), which results in a well-balanced data set suitable for quantitative structure−activity relationship (QSAR) modeling.[35,37−40] One way of performing a SMD is to characterize building blocks (BBs) (i.e., the reactants) using molecular descriptors and then make a subselection based on chemical diversity. The selection yields a reduced BB library that is representative (containing BBs covering most of the variation) of the full library. This process is repeated for all of the different BB sets, and an enumeration of a virtual library of products is made out of the selected BBs. A new diverse selection is made from the product space, lowering the number of compounds to be synthesized. Thus, it is possible to select and synthesize a smaller subset of compounds without losing much of the information contained in the full library. One advantage of making a design in the BB space rather than in the product space is that the interpretation and use of the QSAR will be more direct since the model will give information about desired properties of BBs. The QSAR model, in turn, can be used to predict biological activity for new compounds belonging to the same compound class.[41] Models are established correlating an **X** block of descriptors to a **Y** matrix of responses often using partial least-squares regression to latent structures (PLS).[42,43] Multivariate QSAR models based on PLS also have great value as they allow interpretation of molecular properties important for biological activity. Often, molecular properties (calculated molecular descriptors) are strongly correlated and, hence, cannot serve as design variables in themselves in a multivariate SMD. Instead, variables can be compressed by a multivariate analysis method, typically principal component analysis (PCA),[44] which will result in a low-dimensional hyperplane. The orthogonal principal components constituting the hyperplane, each corresponding to a principal property (e.g., hydrophobicity and size), can be used as design variables in a multivariate SMD. If a design is performed on the basis of BB sets, it is possible to use the principal properties of BBs as variables in a hierarchical PLS (Hi-PLS) analysis.[45] This regression technique gives information about which part of the molecule can be modified to give the desired changes in the responses. Another advantage of this strategy is that it is possible to map regions where the synthetic feasibility is limited, that is, finding regions where building blocks have poor reactivity.

In this paper, we present our design strategy used to select and synthesize analogues to the T3S inhibitor **1a** (Figure 1), identified earlier as a hit in a screening campaign,[19] using three cycles of iterative selection, synthesis, and biological evaluation. Multivariate methods have been utilized to find correlations between biological response and chemical structure. The predictive ability of the models has been evaluated using predictions of three compounds followed by synthesis and biological testing.

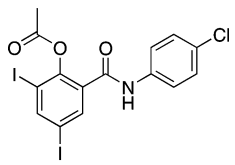

1a

Figure 1. Compound **1a** was identified as a single hit within its class.

2. Results and Discussion

2.1. Establishment of SAR. Six analogues (**1b**, **2a**, **2b**, **3a**, **3b**, and **4**; Table 1) to **1a** were synthesized from readily available starting materials in order to investigate what kind of alterations could be performed on the salicylic ring moiety without losing biological activity entirely. Acetylated salicylanilides were synthesized in two steps. First, the amide was formed from an aniline and a salicylic acid, and in a second step, the product was acetylated using acetic anhydride (see section 2.3 and the Experimental Section for details). The compounds were tested in a T3S-linked reporter gene assay in *Y. pseudotuberculosis*, essentially as described previously (see section 2.4 and the Experimental Section for details).[19] Biological data indicated that the hydroxyl or acetylester group was important to retain biological activity. The iodine at position 3 could be replaced with a hydrogen to increase the activity, but only if the compound was acetylated. If unacetylated, the replacement of iodine at position 3 reduced the activity. If both iodines at the third and fifth positions were replaced with hydrogens, the activity was reduced for both the unacetylated and the acetylated compounds. These initial results supported a further investigation of the SAR as it was possible to modify the structure without total loss of biological activity.

2.2. Library Design using Two Complementary SMDs. The design strategy used was to first perform a SMD to identify regions in chemical space where biologically active compounds could be found and then, in a second cycle, do another SMD around the biologically active compounds to be able to get a more robust QSAR model later on. The first SMD used was a cherry-picking selection from a PCA score plot. The aim was to synthesize a small number of salicylanilides derived from commercially available sets of aniline and salicylic acid derivatives. These were then to be acetylated to yield a second set of compounds. The preliminary knowledge gained from the initial SAR study was used when choosing new BBs, which were manually selected (see Experimental Section). Twenty-five anilines and 22 salicylic acids (see Supporting Information) were used to enumerate a virtual library, resulting in 550 virtual unacetylated salicylanilides. The structural variation of the virtual compounds was summarized with a PCA, and from the resulting three component models ($R^2 = 0.97$, $Q^2 = 0.96$), 16 new unacetylated salicylanilides (**5b**−**20b**) were chosen by visually cherry-picking mainly from the two first principal components (Figure 2a and b). Most of the compounds were chosen around compound **1b** in order to increase the probability that several biologically active compounds would be found. Some of the compounds were chosen in such a way that they should have some BBs in common in order to ensure that the interpretation of results later on would be more straightforward. All of the selected compounds were synthesized (**5b**−**20b**) and, in a second step, acetylated to yield the acetylated salicylanilides

Table 1. Percentile Inhibitions of Luciferase Light Emission for Strain YPIII-pIB29 (*yopE-luxAB*) in the Presence of Compounds **1**−**26** at Four Different Concentrations

ID[a]	Structure	% inhibition of emission [b] (concentrations in μM)				ID	Structure	% inhibition of emission [b] (concentrations in μM)			
		100	50	20	10			100	50	20	10
1a	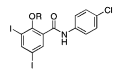	99 ± 0	99 ± 0	98 ± 0	76 ± 1	**14a**	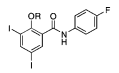	93 ± 2	86 ± 2	76 ± 2	60 ± 4
1b		99 ± 1	100 ± 0	100 ± 0	100 ± 0	**14b**		100 ± 0	99 ± 0	78 ± 1	62 ± 5
2a	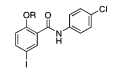	100 ± 0	100 ± 0	100 ± 0	99 ± 2	**15a**	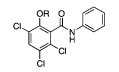	10 ± 5	12 ± 8	-	-
2b		78 ± 6	80 ± 3	85 ± 1	91 ± 1	**15b**		31 ± 3	23 ± 10	21 ± 12	22 ± 14
3a	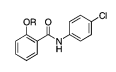	99 ± 1	92 ± 3	44 ± 11	23 ± 4	**16a**	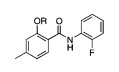	95 ± 1	53 ± 4	8 ± 6	0 ± 3
3b		100 ± 0	99 ± 0	64 ± 4	14 ± 1	**16b**		34 ± 5	35 ± 9	21 ± 11	23 ± 10
4	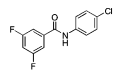	-	-	-	-	**17a**	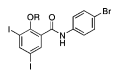	95 ± 1	94 ± 1	86 ± 2	69 ± 4
						17b		100 ± 0	100 ± 0	100 ± 0	100 ± 0
5a	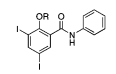	94 ± 1	75 ± 1	48 ± 8	30 ± 6	**18a**	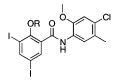	50 ± 7	35 ± 7	19 ± 6	11 ± 7
5b		99 ± 0	87 ± 2	51 ± 3	32 ± 5	**18b**		67 ± 12	57 ± 22	55 ± 16	35 ± 6
6a	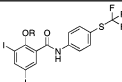	75 ± 1	71 ± 7	71 ± 6	72 ± 8	**19a**	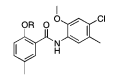	-20 ± 8	-2 ± 11	-	-
6b		100 ± 0	100 ± 0	100 ± 0	83 ± 2	**19b**		-1 ± 5	16 ± 12	-	-
7a	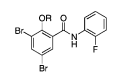	83 ± 6	61 ± 3	15 ± 3	6 ± 3	**20a**	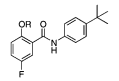	22 ± 6	22 ± 4	37 ± 6	37 ± 5
7b		78 ± 1	64 ± 5	29 ± 1	14 ± 3	**20b**		8 ± 10	13 ± 3	12 ± 4	13 ± 3
8a	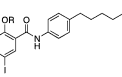	5 ± 5	17 ± 4	19 ± 5	19 ± 5	**21a**	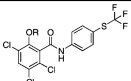	92 ± 5	89 ± 7	95 ± 5	67 ± 7
8b		3 ± 3	22 ± 6	27 ± 12	30 ± 13	**21b**		100 ± 0	100 ± 0	68 ± 3	58 ± 3
9a	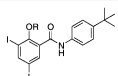	2 ± 15	17 ± 4	20 ± 5	17 ± 5	**22a**	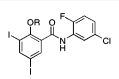	95 ± 1	89 ± 6	58 ± 12	34 ± 3
9b		42 ± 4	41 ± 6	40 ± 4	33 ± 6	**22b**		100 ± 0	100 ± 0	92 ± 2	53 ± 4
10a	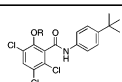	12 ± 13	19 ± 4	7 ± 1	4 ± 12	**23a**	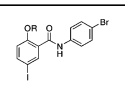	100 ± 0	100 ± 0	100 ± 0	98 ± 2
10b		34 ± 2	23 ± 4	28 ± 13	27 ± 12	**23b**		60 ± 8	62 ± 5	67 ± 7	71 ± 7
11a	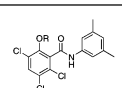	20 ± 8	5 ± 12	6 ± 12	6 ± 15	**24a**	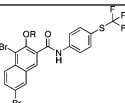	-3 ± 11	4 ± 7	10 ± 4	9 ± 5
11b		52 ± 9	46 ± 7	24 ± 4	21 ± 6	**24b**		63 ± 5	63 ± 6	55 ± 8	41 ± 9
12a	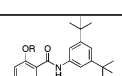	0 ± 5	15 ± 9	-	-	**25a**	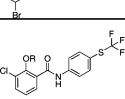	100 ± 0	98 ± 0	70 ± 2	55 ± 2
12b		0 ± 4	-4 ± 3	9 ± 5	12 ± 3	**25b**		100 ± 0	99 ± 0	81 ± 3	61 ± 2
13a	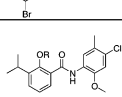	-1 ± 1	4 ± 1	8 ± 4	10 ± 1	**26a**	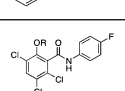	54 ± 4	32 ± 2	23 ± 11	19 ± 15
13b		5 ± 6	19 ± 7	25 ± 8	23 ± 7	**26b**		45 ± 12	32 ± 2	19 ± 8	19 ± 12

[a] For the compound ID's, an **a** denotes R = Ac, and a **b** denotes R = H. [b] Means and standard deviations are calculated from triplicates, and experiments were reproduced on at least two separate occasions. Blank fields correspond to lack of biological activity.

(**5a**−**20a**). All compounds were biologically evaluated in the reporter gene assay, and of the acetylated compounds, 7 (**5a**−**7a**, **14a**, **16a**−**18a**) out of the 16 showed a dose-dependent response. In general, if an acetylated salicylanilide was active, the unacetylated compound was active too.

The second SMD was used as a complement to the cherry-picking selection to get a more robust data set for the QSAR modeling. D-Optimal onion design (DOOD)[46] is an extension to D-optimal designs,[47,48] and a predecessor of this technique was here used to find additional compounds with complementary properties to the ones selected through the cherry-picking SMD. The major advantage of DOOD, compared to traditional D-optimal designs, is that the design can be centered around a compound of your own choice. Around this centerpoint, a number of "onion" layers are chosen, and a D-optimal design is performed within each layer. This approach allows chemical knowledge and experience to play a part in the design process. The design was performed on unacetylated compounds. BBs were characterized with descriptors, and data was compressed with PCA, resulting in three latent variables for both salicylic acids and anilines, explaining 95% ($R^2 = 0.95$, $Q^2 = 0.76$) and 94% ($R^2 = 0.94$, $Q^2 = 0.78$), respectively, of the variation in the matrices. The centerpoint in the design was determined geometrically (see Experimental Section); essentially, a new compound (**22b**) and, from two outer onion layers, five new compounds (**21b**, **23b**, **24b**−**26b**) were selected by the DOOD. Both unacetylated and acetylated versions of the compounds were synthesized and tested (Table 1). Of the six acetylated compounds from the DOOD, five showed biological activity. The only inactive acetylated compound selected by the DOOD (**24a**) was structurally very different from the other compounds. The biologically active acetylated salicylanilides all had IC_{50}

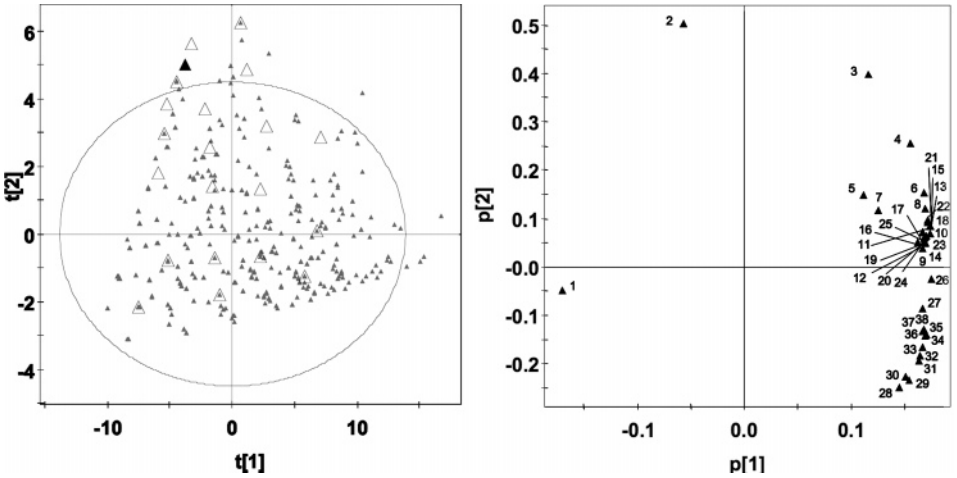

Figure 2. (a) Score plot of 550 virtual salicylanilides. Compound **1b** is marked with a filled triangle, and cherry-picked compounds are marked with an open triangle. (b) Corresponding loading plot of descriptors used.

values below 20 μM, except compound **26a**, which was a low-potency inhibitor. The unacetylated compounds showed a similar biological response as that of the acetylated salicylanilides, except **24b**, which showed an inhibitory effect.

2.3. Synthesis. The acetylated salicylanilides were synthesized in two steps. Anilines and salicylic acids were reacted under microwave heating, using PCl_3 in toluene, to form unacetylated salicylanilides. In a second step, the compounds were acetylated using acetic anhydride and phosphoric acid. The purified compounds were analyzed and characterized with ^{1}H NMR spectroscopy and LC-MS (Experimental Section and Supporting Information). The total yields were 2−60% over two steps. The lower yields in the first step were mainly due to highly deactivated anilines. In the second step, salicylanilides with electron-deficient hydroxyl groups often gave much lower yields than salicylanilides with higher electron density around the hydroxyl group. Poor solubility in the solvent during reaction might have contributed to the poor yields. It was possible to identify trends in the PCA score plot where some regions had products that could not be obtained in any quantifiable amount, while others contained easily synthesized compounds (data not shown). Over three cycles of selection, synthesis and biological evaluation of a total library of 50 analogues to **1a** were synthesized (Table 1). Compound purities, estimated from ^{1}H NMR, are given in a table in the Supporting Information. In addition, purities estimated from LC chromatograms are given for key compounds.

2.4. Biological Evaluation. The biological evaluation was performed using a previously published method.[19,21] In total, 25 acetylated, and the corresponding nonacetylated, salicylanilides were biologically evaluated. The inhibitory effect of the compounds was determined as averages from triplicates in a luminescence assay at four concentrations (100, 50, 20, and 10 μM; Table 1), and the experiments were reproduced on at least two separate occasions. The more potent compounds were tested at four additional concentrations (5, 2, 1, and 0.5 μM; Table 2). Of the 25 acetylated compounds tested, 15 showed a dose-dependent response and thus could be used to establish a multivariate QSAR model. Of these, three came from the SAR study, seven from the cherry-picking selection, and five from the DOOD. Some of the low-activity compounds did not show a dose-dependent response, possibly due to poor solubility, and therefore could not be used in the multivariate modeling later on. The acetylated compounds were more polar than the unacetylated, as indicated by TLC. The increase in lipophilicity was most likely due to the possibility to form an intramolecular hydrogen bond in the nonacetylated compounds. In general, if an acetylated compound was biologically active, its unacetylated counterpart was too, even though there were a few discrepancies (i.e., **24a** and **24b**). Inhibition of protein secretion was investigated through Western analysis for one of the most potent compounds (**23a**) and its unacetylated counterpart (**23b**), and it was found that the level of light emission inhibition roughly

Table 2. Additional Data for the Most Potent Inhibitors, Showing the Luciferase Light Emission Inhibition at Four Different Concentrations

ID	Structure [a]	% inhibition of emission [b] (concentrations in μM)			
		5	2	1	0.5
1a	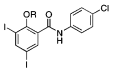	54 ± 1	17 ± 4	7 ± 1	3 ± 2
1b		95 ± 0	60 ± 2	47 ± 1	15 ± 3
2a	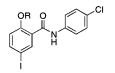	99 ± 0	92 ± 1	73 ± 4	58 ± 4
2b		91 ± 0	90 ± 1	68 ± 4	55 ± 5
6a	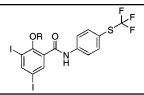	60 ± 2	19 ± 7	11 ± 4	11 ± 4
6b		75 ± 2	39 ± 2	17 ± 1	19 ± 8
14a	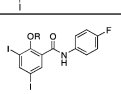	31 ± 2	15 ± 2	6 ± 3	12 ± 2
14b		26 ± 1	6 ± 3	3 ± 1	5 ± 3
17a	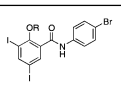	38 ± 5	7 ± 4	8 ± 2	11 ± 3
17b		94 ± 2	74 ± 1	64 ± 1	36 ± 1
21a	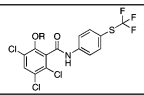	47 ± 7	42 ± 4	15 ± 5	5 ± 4
21b		54 ± 3	18 ± 1	4 ± 3	11 ± 2
22a	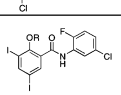	9 ± 3	1 ± 3	1 ± 4	6 ± 4
22b		19 ± 3	6 ± 1	2 ± 1	7 ± 3
23a	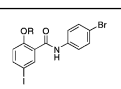	100 ± 0	94 ± 2	71 ± 6	54 ± 4
23b		68 ± 7	68 ± 8	49 ± 4	20 ± 5
25a	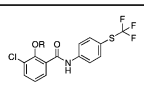	34 ± 4	12 ± 6	6 ± 5	-1 ± 2
25b		38 ± 6	13 ± 5	3 ± 3	-2 ± 5

[a] For the compound ID's, an **a** denotes R = Ac, and a **b** denotes R = H. [b] Means and standard deviations are calculated from triplicates, and experiments were reproduced on at least two separate occasions.

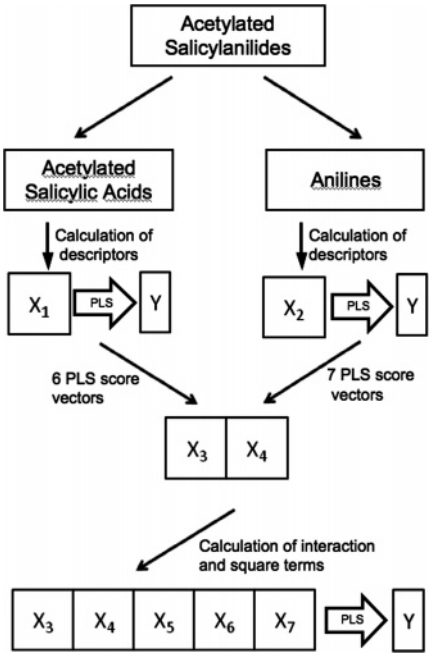

Figure 3. Schematic representation of the multivariate Hi-PLS QSAR model. X_1 and X_2 are the BB data matrices with calculated descriptors, while X_3 and X_4 are the extracted PLS score vectors. X_5 is the square terms of X_3, and X_6 is the square terms of X_4. X_7 is the interaction term between X_3 and X_4.

matched inhibition of protein secretion, as seen for compound **1a** (see Supporting Information).[19]

2.5. Multivariate QSAR for T3S Inhibition. Since a compound could be inactive due to a host of reasons, like efflux and the inability to pass through a membrane, only compounds showing a dose response were used to make a multivariate QSAR model. For the Hi-PLS multivariate QSAR model, the inhibitory values at 20 and 10 μM were used as a multi-**Y** response matrix since the data set had an even spread in biological activity at these concentrations. All of the BBs that were part of an active molecule were assembled in two new tables, one for acetylated salicylic acids and one for anilines. The BBs were characterized with a large number of descriptors, and the **X** blocks were correlated to the multi-**Y** response matrix using PLS, resulting in six PLS score vectors for the salicylic acids ($R_Y^2 = 0.61$, $Q^2 = -0.09$) and seven for the anilines ($R_Y^2 = 0.72$, $Q^2 = 0.28$). Following a number of steps (see Experimental Section), a resulting two-component model ($R_X^2 = 0.34$, $R_Y^2 = 0.96$, $Q^2 = 0.82$) was derived. The procedure is shown in Figure 3. The model showed good correlation between experimental and calculated biological response (Figure 4a and b). A number of attempts were made to establish a multivariate QSAR, using more conventional methods. An attempt using the DOOD parameters for the building blocks was made and did not yield a PLS model, as it only gave a negative value on Q^2. Local PCA models were made on anilines and salicylic acids, and PCA score vectors were extracted and combined into a new data table. However, using the PCA score vectors in a PLS gave the same result as that from using the DOOD parameters. The structural variation found in the PCA models simply did not correlate to the biological response. If a majority of the descriptors have nothing to do with a relevant problem, they introduce noise in which the relevant variables drown. The underlying problem is that it is difficult to decide beforehand which variables are important for the activity. A model could be computed only when correlating properties of the whole molecules to the response using PLS, but only after doing a variable selection. The only way we could establish a model of the BBs correlated to response was by using the methodology outlined above.

Comparing compounds **14a** with **26a** and **5a** with **15a**, it would seem that 3,5,6-trichlorosalicylic acid was a poor BB for making acetylated salicylanilides as T3S inhibitors. Comparing compound **6a** with **21a**, both containing the 4-trifluoromethylsulfanylaniline building block, it became clear that there were interactions between the aniline and the salicylic acid rings which were also supported by the coefficients. The QSAR model could explain complex correlations between structure and activity that, otherwise, would be very difficult to understand due to several nonlinearities, which makes it highly useful for predictions. The biologically active compounds with a high activity generally had an aniline ring moiety with a large-size, highly oval-shaped, high dipole moment and large hydrophobic and negatively charged surfaces. Last, the HOMO and LUMO energies were generally low in the anilines. The salicylic ring moiety in the active molecules with high activity generally had a high dipole moment, high hardness, and high density. Large negative charges, large negatively charged surfaces, and high HOMO energies also characterized a salicylic acid, present in potent inhibitors (e.g compounds **21a** and **23a**; Tables 1 and 2). Even though the model contained several nonlinear terms that, in combination with the PLS score vectors highly correlated nature, made a thorough analysis of the SAR complicated, it could easily be used for predictions of large sets of molecules. A shortcoming of the model was that it could not be used to correctly predict inactive compounds that, in several cases, were predicted as active. This was confirmed by the prediction of the inactive compounds not used in the modeling. The underlying reason is that active and inactive compounds have different molecular properties and the latent variables used to describe the active compounds do not have a relevance for description of the inactive.

2.6. PLS-DA Classification of Inactive and Active Acetylated Salicylanilides. The Hi-PLS multivariate QSAR model was good for predicting and describing the biologically active compounds but not useful for predicting inactive compounds. It was therefore of interest to have a model that could be used to classify active and inactive compounds. To be able to discriminate active from inactive compounds, a PLS-discriminant analysis (PLS-DA)[49] model was made on the acetylated salicylanilides. Twelve out of the 25 compounds (**1a**−**3a**, **5a**−**7a**, **14a**, **16a**−**17a**, **21a**−**23a**, and **25a**) were classified as active (at least 40% T3S inhibition at 50 μM). The same methodology utilized in the Hi-PLS QSAR modeling was used to establish the PLS-DA, using the % light emission inhibition at 50 μM as the response. The correlation of the building blocks to the multi-**Y** response matrix resulted in 11 score vectors for the anilines ($R_X^2 = 1.0$, $R_Y^2 = 0.72$, $Q^2 = -0.27$) and the acetylated salicylic acids ($R_X^2 = 1.0$, $R_Y^2 = 0.62$, $Q^2 = -0.28$). The resulting one-component PLS-DA model ($R_X^2 = 0.19$, $R_Y^2 = 0.75$, $Q^2 = 0.65$) correctly discriminated between the two classes of compounds (Figure 5). The model contained 15 linear terms, 1 square term, and 9 interaction terms (Figure 6). The first score vector for the anilines and the first score vector for the salicylic acids had large positive coefficients and shared a positive interaction term. These terms were the most important, as indicated by the size of their coefficients, and some of the information contained in these terms was also found in the other linear terms. Interpretation of the first linear term of the anilines indicated that the aniline should have high density, rigidity, and

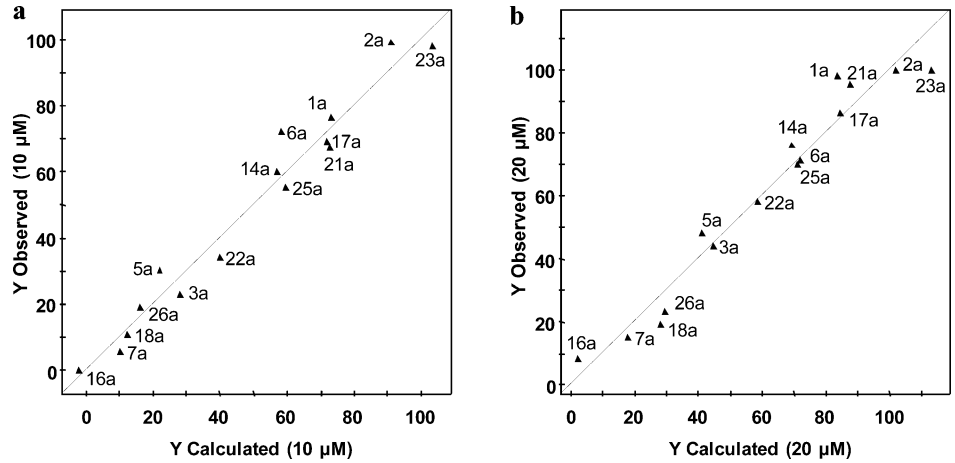

Figure 4. Observed versus calculated plots for (a) 10 and (b) 20 μM compound concentrations, showing good correlations.

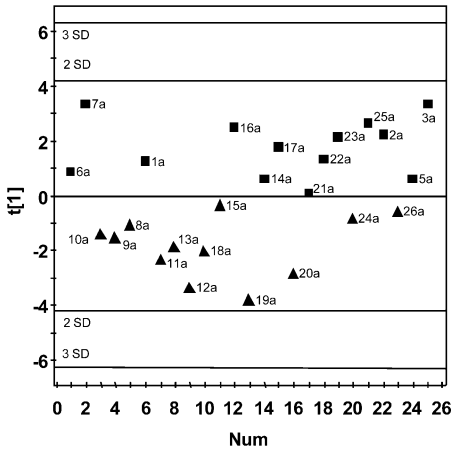

Figure 5. PLS-DA score plot of active (boxes) versus inactive compounds (triangles).

dipole moment, negatively charged surfaces, and low HOMO and LUMO energies. The first linear term of the salicylic acids indicated that in order for the compounds to be active, they should have a salicylic acid with low HOMO, high density, dipole moment, and hardness, and large partial charges. The other main terms had smaller coefficients, but their interaction and square terms had large coefficients, showing that the model contained several nonlinearities.

2.7. External Validation of Models. Three acetylated salicylanilides (**27a**−**29a**; Table 3) were designed and synthesized to validate the multivariate QSAR model and the PLS-DA model. The predicted % inhibition of light emission for the compounds **27a**−**29a** is listed in Table 3. The three compounds were mainly selected based on their predicted T3S inhibitory effect, after 320 compounds had been predicted using both of the multivariate models (see Supporting Information). First, the compounds were predicted, using the PLS-DA model to see if they would be predicted as active. The compounds predicted as active were then predicted using the Hi-PLS multivariate QSAR model. The three compounds chosen for validating the models all had different substitution patterns and different predicted biological activity. Compound **27a** was selected primarily due to the fact that none of the BBs in it had been used in any previously synthesized acetylated salicylanilide and that it was predicted as a potent inhibitor. The PLS-DA model correctly predicted the three compounds to belong to the class of active compounds. The Hi-PLS multivariate QSAR model could correctly rank the three compounds. Compound **28a** was most accurately predicted, and this is most likely due to the fact that the BBs used in the compound had been used in more salicylanilides than the BBs used in **29a**, while compound **27a** did not have any BB present in any salicylanilide that the models were based on.

2.8. Bacterial Growth. Earlier results showed that compound **1a** did not affect growth at concentrations where T3S was completely inhibited.[19] It was previously found that the salicylanilide **1b** affected growth at much lower concentrations than those of **1a**.[25] To verify that the light emission inhibition was due to an effect on the T3S and not on growth, growth experiments were performed on three acetylated compounds (**6a**, **23a**, and **28a**; Tables 1 and 3) and their unacetylated counterparts (**6b**, **23b**, and **28b**; Tables 1 and 3). Growth inhibition was tested on *Y. pseudotuberculosis*, and experiments were reproduced on at least two separate occasions (see Supporting Information). Four of the compounds (**23a**, **23b**, **28a**, and **28b**) did not show any effect on bacterial growth at concentrations at least 10 times higher than their estimated light emission IC_{50} values. Compound **6a** had a slight effect on bacterial growth at 10 μM concentration but not nearly as serious of an effect as that of compound **6b**, which is in accordance with earlier results for **1a** and **1b**.[25] To see if there was any general bacterial growth inhibition, an additional experiment was performed on *Enterotoxigenic Escherichia coli* (ETEC), a Gram-negative bacterium that lacks a T3S system. Growth of ETEC in the absence and presence of the inhibitors was similar to the growth observed in *Y. pseudotuberculosis* (data not shown). The fact that unacetylated salicylanilides have been reported as ATP synthesis inhibitors[50] and that two (**1b** and **6b**) out of four unacetylated compounds tested for growth inhibition showed higher toxicity than their acetylated counterparts led us to focus on the acetylated compounds for the multivariate modeling, as the only interest was on compounds acting on T3S (see discussion in section 2.9.).

2.9. Possible Mode of Action. The bacterial growth experiment results (see section 2.8.) indicated that the acetylated compounds **1a** and **6a** might have had another mode of action than that of the unacetylated compounds **1b** and **6b**, especially considering the fact that unacetylated salicylanilides have been reported to disrupt the proton motive force required for ATP synthesis.[50,51] A low pK_a of the phenol along with electron-withdrawing substituents in both ring systems was important for salicylanilides to be effective proton motive force uncouplers.[50] Looking at the structures of the compounds tested for growth inhibition, the unacetylated compounds with two electron-withdrawing iodines in the salicylic acid ring (**1b** and **6b**) give rise to the most noticeable inhibition. This is probably

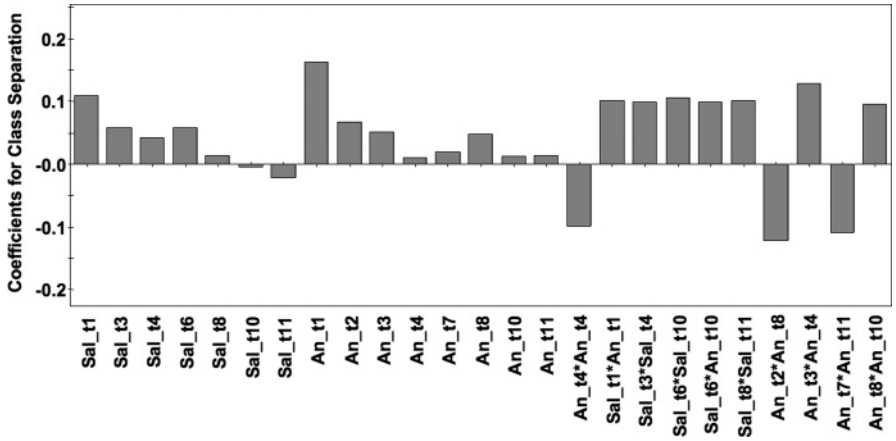

Figure 6. PLS-DA coefficient plot with 15 linear, 1 square, and 9 interaction terms.

Table 3. Luciferase Light Emission Inhibitory Values and Predicted Inhibition for External Test Compounds

ID	Structure [a]	% inhibition of emission [b] (concentrations in μM)								Predicted % inhibition of emission	
		100	50	20	10	5	2	1	0.5	20	10
27a	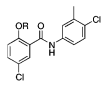	100 ± 0	100 ± 0	100 ± 0	99 ± 0	91 ± 1	62 ± 6	50 ± 2	15 ± 3	76	66
27b		75 ± 14	56 ± 8	85 ± 5	61 ± 20	85 ± 3	62 ± 6	50 ± 2	15 ± 3	-	-
28a	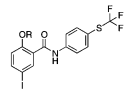	100 ± 0	99 ± 0	74 ± 1	58 ± 0	56 ± 1	80 ± 2	52 ± 2	17 ± 3	64	52
28b		51 ± 2	49 ± 12	57 ± 1	57 ± 2	55 ± 3	53 ± 3	53 ± 4	17 ± 3	-	-
29a	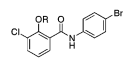	99 ± 0	78 ± 3	36 ± 2	18 ± 1	12 ± 2	9 ± 2	8 ± 2	-2 ± 6	56	41
29b		100 ± 0	96 ± 0	62 ± 1	24 ± 11	12 ± 5	12 ± 3	6 ± 7	5 ± 4	-	-

[a] For the compound ID's, an **a** denotes R = Ac, and a **b** denotes R = H. [b] Means and standard deviations are calculated from triplicates, and experiments were reproduced on at least two separate occasions.

due to the fact that the pK_a should be lower in these compounds and is probably the reason why growth inhibition is not observed for the other compounds tested (**23b** and **28b**). The acetyl group of compounds **1a** and **6a** might be important to circumvent the proton motive force uncoupling, but it is also possible that **1a** and **6a** act as prodrugs and are metabolized into **1b** and **6b**, which have the actual biological effect. It has earlier been reported that unacetylated salicylanilides, with highly similar substitution patterns to those of the compounds presented in this paper, inhibit two-component systems (TCSs) of Gram-positive bacteria.[51] The compounds inhibit TCSs by targeting the sensor kinase and causing aggregation through structural alterations of the kinase.[52] It was shown that the Gram-negative bacteria *E. coli* was effected by the salicylanilides, but only after treating the bacteria with a membrane-permeabilizing agent. After this treatment, it was possible to observe levels of antibacterial activity comparable to those manifested against Gram-positive organisms. These results indicated that Gram-negative bacteria contain the same TCS target as that of the Gram-positive bacteria but that the compounds had problems penetrating the outer membrane. There are a number of TCSs in *Y. pseudotuberculosis*, but to the best of our knowledge, no connection between a TCS and T3S has previously been reported. Interestingly, a link between TCSs and T3S has been established in *Pseudomonas syringae* and *Salmonella*.[53,54]

TCSs control virulence responses of a wide variety of bacterial pathogens.[55] Compounds targeting bacterial virulence have a high chance of having an effect on resistant strains, and there is a possibility that virulence inhibitors will be effective for a long time before resistance becomes an issue. Research on finding new antibacterial agents has traditionally focused on inhibiting bacterial growth through various means (e.g., inhibiting metabolic pathways or disrupting cell wall formation), a strategy not successful in delivering effective novel drugs against diseases caused by resistant pathogens.[56] This highlights the importance of finding and developing inhibitors for novel virulence targets.

3. Conclusions

Using three cycles of iterative selection, synthesis, and biological testing, 50 analogues to **1a** were synthesized and biologically evaluated. First, five compounds (**1b**−**4**) were selected and synthesized as the basis for a preliminary SAR study. The SAR study was followed by a cherry-picking from a PCA score plot that was used to select 16 new unacetylated salicylanilides (**5b**−**20b**), which were synthesized and then acetylated to yield another set of 16 compounds (**5a**−**20a**). In order to ensure a sufficient number of active compounds, a DOOD was utilized to design five new unacetylated salicylanilides (**21b**−**26b**). The compounds from the DOOD were synthesized and, in a second step, acetylated to yield the last five compounds (**21a**−**26a**). After all compounds had been biologically evaluated, a Hi-PLS multivariate QSAR model was established, showing a good correlation between experimental and predicted data for the biologically active acetylated compounds. As a complement to the multivariate QSAR model, a

PLS-DA model was made that could discriminate between active and inactive acetylated compounds. To test the models predictive capability, three new acetylated compounds (**27a**−**29a**) along with their unacetylated counterparts (**27b**−**29b**) were synthesized. Predictions proved to be accurate as the PLS-DA model correctly could predict the compounds to be biologically active, while the multivariate QSAR model could correctly rank the three compounds.

4. Experimental Section

4.1. Cherry-Picking. ChemFinderACX2002Prod[57] was used to search for commercially available salicylic acids and anilines. BBs were chosen manually based on availability, pricing, chemical compatibility, and substitution pattern. Compounds with large substituents at the ortho position to the carboxylic acid were filtered out. The BBs were created in MOE[58] and enumerated to produce a library of 550 virtual products. 1D and 2D descriptors were calculated using the same software (see Supporting Information). The data set was imported to Simca 9.0,[59] and data was centered, unit-variance-scaled, and log-transformed. A PCA was done to compress the data, followed by a variable selection. Data was again centered, unit-variance-scaled, and log-transformed. Variables with low contribution to R^2 and Q^2 were iteratively removed, and the descriptor set was thereby reduced from 110 to 38. The number of significant components in the model was determined by cross validation using seven cross-validation rounds as implemented in Simca 9.0.[59]

4.2. Complementary Design using DOOD. BBs were characterized with 1D and 2D descriptors using MOE (see Supporting Information). The BBs utilized to generate the virtual products for the DOOD were the anilines and salicylic acids employed in the synthesized compounds from the SAR and cherry-picking selections, plus a few additional BBs (see Supporting Information). The descriptors were mainly describing different surfaces, electronic properties, lipophilicity, and size. PCA was performed on both salicylic acids and anilines to compress the variation in the data set. The first three score values (t1, t2, and t3) for each BB group, in combination with the descriptors SlogP and total polar surface area for the entire product, comprised the candidate set variables used for the DOOD selection. The three compounds with the highest biological activity were set as vertices in an inner shell. The middle of the vertices was set as the centerpoint in the design. The candidate set was divided into layers so that the thickness of the two following outer layers was equal to 10% of the thickness of the inner layer. The earlier-synthesized compounds were set as inclusions in the design, and new compounds were selected by the DOOD methodology as applied in an earlier report by Olsson et al.[46]

4.3. Characterization of Building Blocks for Multivariate QSAR Modeling. The BBs were created in MOE, and a rough conformational search was performed by systematically rotating all rotatable bonds 60°. All conformations were energy-minimized with the implemented MMFF94 force field in MOE, and the conformations with the lowest energy were saved. BBs were characterized with a large number of 1D, 2D, and 3D descriptors from MOE in addition to a number of descriptors from Spartan (Linux/Unix 02 edition, AM1 calculations) (see Supporting Information). A PLS regression was made of the data matrices describing the anilines or salicylic acids to the multi-**Y** response matrix in such a way that all BBs were listed together with their inhibition values obtained for the concentrations of 10 and 20 μM. Thus, a BB used in four active compounds would be listed with four different inhibition values. The score vectors were extracted and combined into a new data matrix. A new PLS regression was made to correlate the **X** block to the multi-**Y** matrix. Interaction terms and square terms were calculated, and using a set of rules (see Supporting Information), coefficients were selectively removed.

The cross-validated predicted variation (Q^2) was calculated using seven cross-validation rounds according to

$$Q^2 = 1 - \text{PRESS/SS}$$

where PRESS is the predicted error sum of squares when all objects have been left out once and SS is the total sum of squares of **Y** corrected for the mean.

4.4. PLS-DA. The same methodology, utilizing the exact same pretreatment of BBs and the same descriptor set, was used for the PLS-DA as that in the Hi-PLS MQSAR model. The criterion for activity was set to 40% light emission inhibition at 50 μM. BBs used in all compounds (**1a**−**26b**) were correlated to the response matrix using PLS. After score vector extraction, forming of a new table, and a new PLS regression, square and interaction terms were calculated. Coefficients were removed using another set of rules (see Supporting Information).

4.5. Biological Evaluation, Strains, and Growth Conditions. The biological evaluation was performed with *Yersinia pseudotuberculosis* serotype III (YPIII) strain pIB29 (*yopE-luxAB*).[19] The bacteria were grown at room temperature on LB plates, as described elsewhere.[19,60]

4.6. General Screening and Assay Conditions. The experimental procedures were carried out essentially as described before.[19,21] The *Yersinia pseudotuberculosis* strain YPIII-pIB29 (*yopE-luxAB*) was grown over night in BHI (brain heart infusion) medium containing 5 mM EGTA and 20 mM $MgCl_2$ for calcium depletion at ambient temperature. The optical density at 600 nm was adjusted to 0.15−0.25 in BHI. In parallel, the compounds dissolved in DMSO to be tested were dispensed in four different concentrations (100, 50, 20 and 10 μM final concentration) to the plates manually in triplicate. The final DMSO concentrations in the biological assays were kept at 1% or below. To each well, 50 μL of diluted bacteria was added with a dispenser instrument (Multi Drop, Thermo Lab Systems). The plates were incubated at ambient temperature on a rotary shaker for 1 h, followed by incubation at 37 °C for 2 h. Within 30 min after incubation, 50 μL of fresh decanal solution (10 μL/100 mL water) was added to the wells, and the luciferase activity was measured immediately in the a microplate reader (TECAN GENios, Gain 150; integration time of 20 ms). Experiments were run in triplicate and reproduced on at least two separate occasions.

4.7. Growth Inhibition Experiments. The experimental procedures were carried out as described before.[19,21] Growth inhibition was measured by growing bacteria at 37 °C in the presence of different compound concentrations in 96-well plates containing 100 μL of bacterial culture medium diluted to an OD_{600} of 0.1 in BHI medium with 2.5 mM $CaCl_2$. The experiments were carried out by reading of the absorbance at 595 nm in a TECAN GENios plate reader once an hour and by shaking carried out in a rotary shaker at 37 °C. Growth rates were followed for up to 7 h.

4.8. ETEC Growth Inhibition Experiments. Growth inhibition was measured by growing ETEC bacteria at 37 °C in the presence of different compound concentrations in 96-well plates containing 100 μL of bacterial culture medium diluted to an OD_{600} of 0.1 in LB medium. The experiments were carried out by reading of the absorbance at 595 nm in a TECAN GENios plate reader once an hour and by shaking carried out in a rotary shaker at 37 °C. Growth rates were followed for up to 24 h.

4.9. General Chemistry. ^{1}H NMR spectra were recorded on a Bruker DRX-400 in $CDCl_3$, CD_3OD, or $(CD_3)_2SO$. Mass spectra were recorded by detecting negative (ES^-) molecular ions with an electrospray Waters Micromass ZG 2000 instrument using an XTerra MS C_{18} 5 μm 4.6 × 50 mm column and a H_2O/acetonitrile/formic acid eluent system. The same LC system was also used for purification with a preparative XTerra Prep MS C_{18} 5 μm 19 × 50 mm column and a H_2O/acetonitrile eluent system. Microwave-heated reactions were performed in Emrys process vials (5 mL) using a SmithCreator microwave instrument from Biotage. TLC was performed on Silica gel 60 F_{254} (Merck) with detection by UV light. ^{1}H NMR spectra were recorded using a 400 MHz Bruker spectrometer.

4.10. Typical Procedure for the Formation of Salicylanilides. Salicylic acid (0.7−1.0 mmol, 1 equiv) and aniline (0.8 equiv) were suspended in toluene (5 mL) followed by addition of PCl_3 (1 equiv). The reaction was performed using a microwave instrument at

150 °C for 10 min. The reaction mixture was dissolved with EtOAc, washed with water followed by $NaHCO_3$ (aq., sat.), and extracted with EtOAc. The organic phase was dried using anhydrous $MgSO_4$ and filtered. After absorption onto silica gel, the crude products were purified using flash chromatography with heptane/EtOAc as the eluent.

4.11. Typical Procedure for Acetylation of Salicylanilides. To a round-bottom flask (25 mL) containing the salicylanilide, excess of acetic acid anhydride (15 mL) and a few droplets of phosphoric acid (85%, aq.) were added. The reaction was performed at 70 °C for 1 h. Addition of ice and water under cooling generally resulted in a precipitate of the product. Flash chromatography (silica gel using heptane/EtOAc systems as the eluent) or preparative LC-MS was used if no pure precipitate of the product could be isolated. Compound purities, estimated from ^{1}H NMR and LC UV traces, are given in the Supporting Information.

***N*-(4-Chlorophenyl)-2-acetoxy-3,5-diiodobenzamide (1a).** ^{1}H NMR (DMSO): δ 10.55 (s, 1H), 8.38 (d, J = 2.0 Hz, 1H), 7.99 (d, J = 2.0 Hz, 1H), 7.71−7.64 (m, 2H), 7.43−7.37 (m, 2H), 2.23 (s, 3H). LCMS (*m*/*z*): [M − H$^-$]$^-$ calcd for [$C_{15}H_{10}ClI_2NO_3$], 539.84; found [−Ac$^+$], 497.77.

***N*-(4-Chlorophenyl)-2-hydroxy-3,5-diiodobenzamide (1b).** ^{1}H NMR (DMSO): δ 13.02 (bs, 1H), 10.89 (bs, 1H), 8.35 (d, J = 1.9 Hz, 1H), 8.21 (d, J = 1.9 Hz, 1H), 7.73−7.68 (m, 2H), 7.49−7.43 (m, 2H). LCMS (*m*/*z*): [M − H$^-$]$^-$ calcd for [$C_{13}H_8ClI_2NO_2$], 497.83; found, 497.92.

***N*-(4-Chlorophenyl)-2-acetoxy-5-iodobenzamide (2a).** ^{1}H NMR ($CDCl_3$): δ 8.13 (d, J = 2.1 Hz, 1H), 7.96 (bs, 1H), 7.82 (dd, J = 2.2 Hz, 8.5 Hz, 1H), 7.53 (d, J = 8.8 Hz, 1H), 7.38−7.30 (m, 2H), 6.92 (d, J = 8.5 Hz, 1H), 2.32 (s, 3H). LCMS (*m*/*z*): [M − H$^-$]$^-$ calcd for [$C_{15}H_{11}ClINO_3$], 413.94; found [−Ac$^+$], 372.02.

***N*-(4-Chlorophenyl)-2-hydroxy-5-iodobenzamide (2b).** ^{1}H NMR (DMSO): δ 11.70 (bs, 1H), 10.62 (bs, 1H), 8.15 (d, J = 1.9 Hz, 1H), 7.77−7.66 (m, 3H), 7.46−7.40 (m, 2H), 6.81 (d, J = 8.4 Hz, 1H). LCMS (*m*/*z*): [M − H$^-$]$^-$ calcd for [$C_{13}H_9ClINO_2$], 371.93; found, 372.02.

***N*-(4-Chlorophenyl)-2-acetoxybenzamide (3a).** ^{1}H NMR ($CDCl_3$): δ 8.01 (s, 1H), 7.84 (d, J = 7.6 Hz, 1H), 7.60−7.50 (m, 3H), 7.41−7.30 (m, 3H), 7.16 (d, J = 8.1 Hz, 1H), 2.33 (s, 3H). LCMS (*m*/*z*): [M − H$^-$]$^-$ calcd for [$C_{15}H_{12}ClNO_3$], 288.04; found [−Ac$^+$], 246.11.

***N*-(4-Chlorophenyl)-2-hydroxybenzamide (3b).** ^{1}H NMR (DMSO): δ 11.63 (bs, 1H), 10.49 (s, 1H), 7.95−7.90 (m, 1H), 7.80−7,73 (m, 2H), 7.46−7.40 (m, 3H), 7.01−6.93 (m, 2H). LCMS (*m*/*z*): [M − H$^-$]$^-$ calcd for [$C_{13}H_{10}ClNO_2$], 246.03; found, 246.11.

***N*-(4-Chlorophenyl)-3,5-difluorobenzamide (4).** ^{1}H NMR (DMSO): δ 10.48 (s, 1H), 7.82−7.77 (m, 2H), 7.71−7.64 (m, 2H), 7.58−7.59 (m, 1H), 7.46−7.41 (m, 2H). LCMS (*m*/*z*): [M − H$^-$]$^-$ calcd for [$C_{13}H_8ClF_2NO$], 266.02; found, 266.10.

***N*-Phenyl-2-acetoxy-3,5-diiodobenzamide (5a).** ^{1}H NMR ($CDCl_3$): δ 8.26 (d, J = 2.1 Hz, 1H), 8.02 (d, J = 2.0 Hz, 1H), 7.73 (s, 1H), 7.56 (d, J = 8.2 Hz, 2H), 7.40−7.34 (m, 2H), 7.19−7.15 (m, 1H), 2.37 (s, 3H). LCMS (*m*/*z*): [M − H$^-$]$^-$ calcd for [$C_{15}H_{11}I_2NO_3$], 505.87; found [−Ac$^+$], 463.97.

***N*-Phenyl-2-hydroxy-3,5-diiodobenzamide (5b).** ^{1}H NMR (DMSO): δ 13.24 (bs, 1H), 10.77 (bs, 1H), 8.39 (d, J = 1.9 Hz, 1H), 8.21 (d, J = 1.8 Hz, 1H), 7.70−7.63 (m, 2H), 7.44−7.36 (m, 2H), 7.22−7.16 (m, 1H). LCMS (*m*/*z*): [M − H$^-$]$^-$ calcd for [$C_{13}H_9I_2NO_2$], 463.86; found, 463.89.

***N*-(4-Trifluoromethylsulfanylphenyl)-2-acetoxy-3,5-diiodobenzamide (6a).** ^{1}H NMR ($CDCl_3$): δ 8.29 (d, J = 2.1 Hz, 1H), 8.00 (d, J = 2.1 Hz, 1H), 7.88 (s, 1H), 7.70−7.61 (m, 4H), 2.38 (s, 3H). LCMS (*m*/*z*): [M − H$^-$]$^-$ calcd for [$C_{16}H_{10}F_3I_2NO_3S$], 605.83; found [−Ac$^+$], 563.93.

***N*-(4-Trifluoromethylsulfanylphenyl)-2-hydroxy-3,5-diiodobenzamide (6b).** ^{1}H NMR (DMSO): δ 12.73 (bs, 1H), 10.99 (bs, 1H), 8.33 (d, J = 1.8 Hz, 1H), 8.23 (d, J = 1.6 Hz, 1H), 7.85 (d, J = 8.7 Hz, 2H), 7.75 (d, J = 8.7 Hz, 2H). LCMS (*m*/*z*): [M − H$^-$]$^-$ calcd for [$C_{14}H_8F_3I_2NO_2S$], 563.82; found, 563.74.

***N*-(2-Fluorophenyl)-2-acetoxy-3,5-dibromobenzamide (7a).** ^{1}H NMR ($CDCl_3$): δ 8.47−8.34 (m, 2H), 8.05 (s, 1H), 7.91 (s, 1H), 7.24−7.08 (m, 3H), 2.43 (s, 3H). LCMS (*m*/*z*): [M − H$^-$]$^-$ calcd for [$C_{15}H_{10}Br_2FNO_3$], 427.89; found [−Ac$^+$], 385.99.

***N*-(2-Fluorophenyl)-3,5-dibromo-2-hydroxybenzamide (7b).** ^{1}H NMR (DMSO): δ 10.91 (bs, 1H), 8.28 (d, J = 2.3 Hz, 1H), 8.04 (d, J = 2.2 Hz, 1H), 7.68−7.61 (m, 1H), 7.39−7.31 (m, 2H), 7.30−7.24 (m, 1H). LCMS (*m*/*z*): [M − H$^-$]$^-$ calcd for [$C_{13}H_8Br_2FNO_2$], 385.88; found, 386.03.

***N*-(4-Heptylphenyl)-2-acetoxy-3,5-diiodobenzamide (8a).** ^{1}H NMR (DMSO): δ 10.34 (s, 1H), 8.36 (d, J = 2.0 Hz, 1H), 7.96 (d, J = 2.0 Hz, 1H), 7.53 (d, J = 8.5 Hz, 2H), 7.15 (d, J = 8.5 Hz, 2H), 2.57−2.49 (m, 2H), 2.23 (s, 3H), 1.63−1.47 (m, 2H), 1.36−1.17 (m, 8H), 0.92−0.79 (m, 3H). LCMS (*m*/*z*): [M − H$^-$]$^-$ calcd for [$C_{22}H_{25}I_2NO_3$], 603.98; found [−Ac$^+$], 562.09.

***N*-(4-Heptylphenyl)-2-hydroxy-3,5-diiodobenzamide (8b).** ^{1}H NMR ($CDCl_3$): δ 12.90 (s, 1H), 8.18 (s, 1H), 7.84 (s, 1H), 7.77 (s, 1H), 7.44 (d, J = 8.1 Hz, 2H), 7.23 (d, J = 8.1 Hz, 2H), 2.65−2.56 (m, 2H), 1.67−1.53 (m, 2H), 1.39−1.28 (m, 8H), 0.93−0.83 (m, 3H). LCMS (*m*/*z*): [M − H$^-$]$^-$ calcd for [$C_{20}H_{23}I_2NO_2$], 561.97; found, 562.09.

***N*-(4-*tert*-Butylphenyl)-2-acetoxy-3,5-diiodobenzamide (9a).** ^{1}H NMR ($CDCl_3$): δ 8.25 (s, 1H), 8.01 (s, 1H), 7.70 (s, 1H), 7.47 (d, J = 8.3 Hz, 2H), 7.38 (d, J = 8.4 Hz, 2H), 2.37 (s, 3H), 1.32 (s, 9H). LCMS (*m*/*z*): [M − H$^-$]$^-$ calcd for [$C_{19}H_{19}I_2NO_3$], 561.94; found [−Ac$^+$], 520.04.

***N*-(4-*tert*-Butylphenyl)-2-hydroxy-3,5-diiodobenzamide (9b).** ^{1}H NMR ($CDCl_3$): δ 12.91 (s, 1H), 8.19 (s, 1H), 7.84 (s, 1H), 7.77 (s, 1H), 7.51−7.39 (m, 4H), 1.33 (s, 9H). LCMS (*m*/*z*): [M − H$^-$]$^-$ calcd for [$C_{17}H_{17}I_2NO_2$], 519.93; found, 520.04.

***N*-(4-*tert*-Butylphenyl)-2-acetoxy-3,5,6-trichlorobenzamide (10a).** ^{1}H NMR (DMSO): δ 10.64 (s, 1H), 8.19 (s, 1H), 7.58−7.49 (m, 2H), 7.41−7.34 (m, 2H), 2.26 (s, 3H), 1.27 (s, 9H). LCMS (*m*/*z*): [M − H$^-$]$^-$ calcd for [$C_{19}H_{18}Cl_3NO_3$], 412.03; found [−Ac$^+$], 370.10.

***N*-(4-*tert*-Butylphenyl)-3,5,6-trichloro-2-hydroxybenzamide (10b).** ^{1}H NMR (DMSO): δ 10.56 (bs, 1H), 10.49 (s, 1H), 7.84 (s, 1H), 7.60−7.56 (m, 2H), 7.39−7.34 (m, 2H), 1.27 (s, 9H). LCMS (*m*/*z*): [M − H$^-$]$^-$ calcd for [$C_{17}H_{16}Cl_3NO_2$], 370.02; found, 370.10.

***N*-(3,5-Dimethylphenyl)-2-acetoxy-3,5,6-trichlorobenzamide (11a).** ^{1}H NMR ($CDCl_3$): δ 7.64 (s, 1H), 7.34 (s, 1H), 7.19 (s, 2H), 6.84 (s, 1H), 2.33 (s, 6H), 2.30 (s, 3H). LCMS (*m*/*z*): [M − H$^-$]$^-$ calcd for [$C_{17}H_{14}Cl_3NO_3$], 384.00; found [−Ac$^+$], 342.06.

***N*-(3,5-Dimethylphenyl)-3,5,6-trichloro-2-hydroxybenzamide (11b).** ^{1}H NMR (DMSO): δ 10.55 (bs, 1H), 10.42 (bs, 1H), 7.83 (s, 1H), 7.29 (s, 2H), 6.76 (s, 1H), 2.25 (s, 6H). LCMS (*m*/*z*): [M − H$^-$]$^-$ calcd for [$C_{15}H_{12}Cl_3NO_2$], 341.99; found, 342.06.

***N*-(3,5-Di-*tert*-butylphenyl)-2-acetoxy-5-bromobenzamide (12a).** ^{1}H NMR ($CDCl_3$): δ 8.09−7.92 (m, 2H), 7.61 (dd, J = 2.4 Hz, 8.6 Hz, 1H), 7.44 (s, 2H), 7.26−7.24 (m, 1H), 7.06 (d, J = 8.6 Hz, 1H), 2.35 (s, 3H), 1.34 (s, 18H). LCMS (*m*/*z*): [M − H$^-$]$^-$ calcd for [$C_{23}H_{28}BrNO_3$], 444.12; found [−Ac$^+$], 402.07.

***N*-(3,5-Di-*tert*-butylphenyl)-5-bromo-2-hydroxybenzamide (12b).** ^{1}H NMR ($CDCl_3$): δ 7.85 (s, 1H), 7.66 (d, J = 2.3 Hz, 1H), 7.51 (dd, J = 2.3 Hz, 8.9 Hz, 1H), 7.42 (d, J = 1.6 Hz, 2H), 7.31−7.29 (m, 1H), 6.93 (d, J = 8.9 Hz, 1H), 1.35 (s, 18H). LCMS (*m*/*z*): [M − H$^-$]$^-$ calcd for [$C_{21}H_{26}BrNO_2$], 402.11; found, 402.22.

***N*-(4-Chloro-2-methoxy-5-methylphenyl)-2-acetoxy-3-isopropylbenzamide (13a).** ^{1}H NMR ($CDCl_3$): δ 8.42 (s, 1H), 8.37 (s, 1H), 7.64−7.58 (m, 1H), 7.50−7.45 (m, 1H), 7.33 (t, J = 7.7 Hz, 1H), 6.88 (s, 1H), 3.87 (s, 3H), 3.10−3.01 (m, 1H), 2.34 (s, 3H), 2.32 (s, 3H), 1.25 (s, 3H), 1.23 (s, 3H). LCMS (*m*/*z*): [M − H$^-$]$^-$ calcd for [$C_{20}H_{22}ClNO_4$], 374.05; found [−Ac$^+$], 332.22.

***N*-(4-Chloro-2-methoxy-5-methylphenyl)-2-hydroxy-3-isopropylbenzamide (13b).** ^{1}H NMR ($CDCl_3$): δ 8.55 (s, 1H), 8.29 (s, 1H), 7.42−7.33 (m, 2H), 6.94−6.85 (m, 2H), 3.92 (s, 3H), 3.48−3.35 (m, 1H), 2.36 (s, 3H), 1.26 (s, 3H), 1.25 (s, 3H). LCMS (*m*/*z*): [M − H$^-$]$^-$ calcd for [$C_{18}H_{20}ClNO_3$], 332.11; found, 332.29.

***N*-(4-Fluorophenyl)-2-acetoxy-3,5-diiodobenzamide (14a).** ^{1}H NMR (DMSO): δ 10.48 (s, 1H), 8.38 (d, J = 2.0 Hz, 1H), 7.99

(d, $J = 2.1$ Hz, 1H), 7.71−7.64 (m, 2H), 7.23−7.15 (m, 2H), 2.23 (s, 3H). LCMS (*m*/*z*): $[M - H^-]^-$ calcd for $[C_{15}H_{10}FI_2NO_3]$, 523.87; found $[-Ac^+]$, 481.96.

***N*-(4-Fluorophenyl)-2-hydroxy-3,5-diiodobenzamide (14b).** ^{1}H NMR (MeOD): δ 8.27 (d, $J = 2.0$ Hz, 1H), 8.19 (d, $J = 2.0$ Hz, 1H), 7.68−7.63 (m, 2H), 7.15−7.07 (m, 2H). LCMS (*m*/*z*): $[M - H^-]^-$ calcd for $[C_{13}H_8FI_2NO_2]$, 481.85; found, 481.96.

***N*-Phenyl-2-acetoxy-3,5,6-trichlorobenzamide (15a).** ^{1}H NMR (MeOD): δ 7.89 (s, 1H), 7.61 (d, $J = 7.9$ Hz, 2H), 7.42−7.32 (m, 2H), 7.23−7.13 (m, 1H), 2.30 (s, 3H). LCMS (*m*/*z*): $[M - H^-]^-$ calcd for $[C_{15}H_{10}Cl_3NO_3]$, 355.96; found $[-Ac^+]$, 314.07.

***N*-Phenyl-3,5,6-trichloro-2-hydroxybenzamide (15b).** ^{1}H NMR (DMSO): δ 10.84−10.49 (m, 2H), 7.83 (s, 1H), 7.71−7.65 (m, 2H), 7.38−7.32 (m, 2H), 7.14−7.08 (m, 1H). LCMS (*m*/*z*): $[M - H^-]^-$ calcd for $[C_{13}H_8Cl_3NO_2]$, 313.95; found, 314.05.

***N*-(2-Fluorophenyl)-2-acetoxy-4-methylbenzamide (16a).** ^{1}H NMR ($CDCl_3$): δ 8.74 (s, 1H), 8.58−8.49 (m, 1H), 7.97 (d, $J = 7.9$ Hz, 1H), 7.22−7.04 (m, 4H), 7.01 (s, 1H), 2.42 (s, 3H), 2.41 (s, 3H). LCMS (*m*/*z*): $[M - H^-]^-$ calcd for $[C_{16}H_{14}FNO_3]$, 286.09; found $[-Ac^+]$, 244.21.

***N*-(2-Fluorophenyl)-2-hydroxy-4-methylbenzamide (16b).** ^{1}H NMR (DMSO): δ 11.87 (bs, 1H), 10.67 (s, 1H), 8.23−8.16 (m, 1H), 7.91 (d, $J = 8.0$ Hz, 1H), 7.35−7.28 (m, 1H), 7.26−7.14 (m, 2H), 6.86−6.78 (m, 2H), 2.30 (s, 3H). LCMS (*m*/*z*): $[M - H^-]^-$ calcd for $[C_{14}H_{12}FNO_2]$, 244.08; found, 244.16.

***N*-(4-Bromophenyl)-2-acetoxy-3,5-diiodobenzamide (17a).** ^{1}H NMR ($CDCl_3$): δ 8.27 (s, 1H), 7.99 (s, 1H), 7.74 (s, 1H), 7.52−7.41 (m, 4H), 2.36 (s, 3H). LCMS (*m*/*z*): $[M - H^-]^-$ calcd for $[C_{15}H_{10}BrI_2NO_3]$, 583.79; found $[-Ac^+]$, 541.70.

***N*-(4-Bromophenyl)-2-hydroxy-3,5-diiodobenzamide (17b).** ^{1}H NMR (DMSO): δ 12.98 (bs, 1H), 10.73 (bs, 1H), 8.36 (d, $J = 2.0$ Hz, 1H), 8.23 (d, $J = 1.9$ Hz, 1H), 7.68−7.63 (m, 2H), 7.62−7.56 (m, 2H). LCMS (*m*/*z*): $[M - H^-]^-$ calcd for $[C_{13}H_8BrI_2NO_2]$, 541.77; found, 541.85.

***N*-(4-Chloro-2-methoxy-5-methylphenyl)-2-acetoxy-3,5-diiodobenzamide (18a).** ^{1}H NMR ($CDCl_3$): δ 8.45 (s, 1H), 8.36 (s, 1H), 8.27 (d, $J = 2.1$ Hz, 1H), 8.12 (d, $J = 2.0$ Hz, 1H), 6.90 (s, 1H), 3.89 (s, 3H), 2.37 (s, 3H), 2.34 (s, 3H). LCMS (*m*/*z*): $[M - H^-]^-$ calcd for $[C_{17}H_{14}ClI_2NO_4]$, 583.86; found $[-Ac^+]$, 541.77.

***N*-(4-Chloro-2-methoxy-5-methylphenyl)-2-hydroxy-3,5-diiodobenzamide (18b).** ^{1}H NMR (DMSO): δ 13.18 (bs, 1H), 10.50 (bs, 1H), 8.39 (s, 1H), 8.23 (s, 1H), 7.53 (s, 1H), 7.19 (s, 1H), 3.82 (s, 3H), 2.27 (s, 3H). LCMS (*m*/*z*): $[M - H^-]^-$ calcd for $[C_{15}H_{12}ClI_2NO_3]$, 541.85; found, 542.00.

***N*-(4-Chloro-2-methoxy-5-methylphenyl)-2-acetoxy-5-methylbenzamide (19a).** ^{1}H NMR ($CDCl_3$): δ 8.76 (s, 1H), 8.47 (s, 1H), 7.77 (d, $J = 2.0$ Hz, 1H), 7.34−7.29 (m, 1H), 7.04 (d, $J = 8.2$ Hz, 1H), 6.90 (s, 1H), 3.89 (s, 3H), 2.41 (s, 3H), 2.36 (s, 3H), 2.34 (s, 3H). LCMS (*m*/*z*): $[M - H^-]^-$ calcd for $[C_{18}H_{18}ClNO_4]$, 346.08; found $[-Ac^+]$, 304.20.

***N*-(4-Chloro-2-methoxy-5-methylphenyl)-2-hydroxy-5-methylbenzamide (19b).** ^{1}H NMR (DMSO): δ 11.45 (s, 1H), 10.79 (s, 1H), 8.39 (s, 1H), 7.81 (d, $J = 2.0$ Hz, 1H), 7.26−7.20 (m, 1H), 7.14 (s, 1H), 6.20 (d, $J = 8.3$ Hz, 1H), 3.88 (s, 3H), 2.28 (s, 3H), 2.27 (s, 3H). LCMS (*m*/*z*): $[M - H^-]^-$ calcd for $[C_{16}H_{16}ClNO_3]$, 304.07; found, 304.15.

***N*-(4-*tert*-Butylphenyl)-2-acetoxy-5-fluorobenzamide (20a).** ^{1}H NMR ($CDCl_3$): δ 8.01 (s, 1H), 7.58 (dd, $J = 2.9$ Hz, 5.5 Hz, 1H), 7.54−7.48 (m, 2H), 7.42−7.37 (m, 2H), 7.24−7.17 (m, 1H), 7.16−7.11 (m, 1H), 2.34 (s, 3H), 1.32 (s, 9H). LCMS (*m*/*z*): $[M - H^-]^-$ calcd for $[C_{19}H_{20}FNO_3]$, 328.13; found $[-Ac^+]$, 286.25.

***N*-(4-*tert*-Butylphenyl)-5-fluoro-2-hydroxybenzamide (20b).** ^{1}H NMR (DMSO): δ 12.99 (bs, 1H), 7.63−7.53 (m, 3H), 7.33 (d, $J = 8.6$ Hz, 2H), 7.08−7.00 (m, 1H), 6.74−6.66 (m, 1H), 1.28 (s, 9H). LCMS (*m*/*z*): $[M - H^-]^-$ calcd for $[C_{17}H_{18}FNO_2]$, 286.12; found, 286.25.

***N*-(4-Trifluoromethylsulfanylphenyl)-2-acetoxy-3,5,6-trichlorobenzamide (21a).** ^{1}H NMR (DMSO): δ 11.12 (s, 1H), 8.24 (s, 1H), 7.82−7.71 (m, 4H), 2.27 (s, 3H). LCMS (*m*/*z*): $[M - H^-]^-$ calcd for $[C_{16}H_9Cl_3F_3NO_3S]$, 455.92; found $[-Ac^+]$, 413.98.

***N*-(4-Trifluoromethylsulfanylphenyl)-3,5,6-trichloro-2-hydroxybenzamide (21b).** ^{1}H NMR (DMSO): δ 10.97 (bs, 1H), 10.74 (s, 1H), 7.88 (s, 1H), 7.86−7.80 (m, 2H), 7.75−7.70 (m, 2H). LCMS (*m*/*z*): $[M - H^-]^-$ calcd for $[C_{14}H_7Cl_3F_3NO_2S]$, 413.91; found, 413.98.

***N*-(5-Chloro-2-fluorophenyl)-2-acetoxy-3,5-diiodobenzamide (22a).** ^{1}H NMR ($CDCl_3$): δ 8.50 (d, $J = 6.2$ Hz, 1H), 8.31 (s, 1H), 8.28 (s, 1H), 8.17 (s, 1H), 7.13−7.04 (m, 2H), 2.42 (s, 3H). LCMS (*m*/*z*): $[M - H^-]^-$ calcd for $[C_{15}H_9ClFI_2NO_3]$, 557.83; found $[-Ac^+]$, 515.76.

***N*-(5-Chloro-2-fluorophenyl)-2-hydroxy-3,5-diiodobenzamide (22b).** ^{1}H NMR (MeOD): δ 8.31−8.18 (m, 2H), 7.89−7.80 (m, 1H), 7.31−7.17 (m, 2H). LCMS (*m*/*z*): $[M - H^-]^-$ calcd for $[C_{13}H_7ClFI_2NO_2]$, 515.82; found, 515.76.

***N*-(4-Bromophenyl)-2-acetoxy-5-iodobenzamide (23a).** ^{1}H NMR (DMSO): δ 10.53 (s, 1H), 7.99 (d, $J = 2.0$ Hz, 1H), 7.95−7.89 (m, 1H), 7.65 (d, $J = 8.9$ Hz, 2H), 7.53 (d, $J = 8.9$ Hz, 2H), 7.09 (d, $J = 8.5$ Hz, 1H), 2.18 (s, 3H). LCMS (*m*/*z*): $[M - H^-]^-$ calcd for $[C_{15}H_{11}BrINO_3]$, 457.89; found $[-Ac^+]$, 416.00.

***N*-(4-Bromophenyl)-2-hydroxy-5-iodobenzamide (23b).** ^{1}H NMR (DMSO): δ 11.70 (bs, 1H), 10.61 (bs, 1H), 8.14 (d, $J = 2.2$ Hz, 1H), 7.73−7.65 (m, 3H), 7.58−7.53 (m, 2H), 6.81 (d, $J = 8.8$ Hz, 1H). LCMS (*m*/*z*): $[M - H^-]^-$ calcd for $[C_{13}H_9BrINO_2]$, 415.88; found, 416.00.

***N*-(4-Trifluoromethylsulfanylphenyl)-2-acetoxy-3,7-dibromonaphthamide (24a).** ^{1}H NMR (DMSO): δ 10.99 (s, 1H), 8.50 (d, $J = 2.0$ Hz, 1H), 8.42 (s, 1H), 8.17 (d, $J = 9.0$ Hz, 1H), 7.97 (dd, $J = 2.0$ Hz, 9.0 Hz, 1H), 7.92−7.85 (m, 2H), 7.78−7.72 (m, 2H), 2.32 (s, 3H). LCMS (*m*/*z*): $[M - H^-]^-$ calcd for $[C_{20}H_{12}Br_2F_3NO_3S]$, 559.88; found $[-Ac^+]$, 517.94.

***N*-(4-Trifluoromethylsulfanylphenyl)-3,7-dibromo-2-hydroxynaphthamide (24b).** ^{1}H NMR (DMSO): δ 11.52 (bs, 1H), 11.17 (bs, 1H), 8.50 (s, 1H), 8.26 (d, $J = 2.0$ Hz, 1H), 8.01 (d, $J = 9.1$ Hz, 1H), 7.95−7.89 (m, 2H), 7.83 (dd, $J = 2.0$ Hz, 9.1 Hz, 1H), 7.80−7.74 (m, 2H). LCMS (*m*/*z*): $[M - H^-]^-$ calcd for $[C_{18}H_{10}Br_2F_3NO_2S]$, 517.87; found, 517.94.

***N*-(4-Trifluoromethylsulfanylphenyl)-2-acetoxy-3-chlorobenzamide (25a).** ^{1}H NMR ($CDCl_3$): δ 8.04 (s, 1H), 7.68−7.59 (m, 6H), 7.37−7.28 (m, 1H), 2.38 (s, 3H). LCMS (*m*/*z*): $[M - H^-]^-$ calcd for $[C_{16}H_{11}ClF_3NO_3S]$, 388.00; found $[-Ac^+]$, 346.08.

***N*-(4-Trifluoromethylsulfanylphenyl)-3-chloro-2-hydroxybenzamide (25b).** ^{1}H NMR (DMSO): δ 12.25 (s, 1H), 10.84 (s, 1H), 7.96 (d, $J = 8.8$ Hz, 1H), 7.89 (d, $J = 8.6$ Hz, 2H), 7.75 (d, $J = 8.6$ Hz, 2H), 7.67 (d, $J = 8.8$ Hz, 1H), 7.06−6.97 (m, 1H). LCMS (*m*/*z*): $[M - H^-]^-$ calcd for $[C_{14}H_9ClF_3NO_2S]$, 345.99; found, 346.09.

***N*-(4-Fluorophenyl)-2-acetoxy-3,5,6-trichlorobenzamide (26a).** ^{1}H NMR ($CDCl_3$): δ 7.66 (s, 1H), 7.56−7.48 (m, 2H), 7.43 (s, 1H), 7.12−7.03 (m, 2H), 2.30 (s, 3H). LCMS (*m*/*z*): $[M - H^-]^-$ calcd for $[C_{15}H_9Cl_3FNO_3]$, 373.96; found $[-Ac^+]$, 332.06.

***N*-(4-Fluorophenyl)-3,5,6-trichloro-2-hydroxybenzamide (26b).** ^{1}H NMR (DMSO): δ 7.76−7.59 (m, 3H), 7.24−7.11 (m, 2H). LCMS (*m*/*z*): $[M - H^-]^-$ calcd for $[C_{13}H_7Cl_3FNO_2]$, 331.94; found, 332.01.

***N*-(4-Chloro-3-methylphenyl)-2-acetoxy-5-chlorobenzamide (27a).** ^{1}H NMR ($CDCl_3$): δ 7.94 (s, 1H), 7.80 (d, $J = 2.5$ Hz, 1H), 7.51 (s, 1H), 7.47 (dd, $J = 8.7$ Hz, 6.1 Hz, 1H), 7.35−7.30 (m, 2H), 7.11 (d, $J = 8.7$ Hz, 1H), 2.38 (s, 3H), 2.33 (s, 3H). LCMS (*m*/*z*): $[M - H^-]^-$ calcd for $[C_{16}H_{13}Cl_2NO_3]$, 336.02; found $[-Ac^+]$, 294.04.

***N*-(4-Chloro-3-methylphenyl)-5-chloro-2-hydroxybenzamide (27b).** ^{1}H NMR (DMSO): δ 11.75 (bs, 1H), 10.49 (s, 1H), 7.92 (d, $J = 2.7$ Hz, 1H), 7.70 (d, $J = 2.2$ Hz, 1H), 7.58 (dd, $J = 2.4$ Hz, 8.6 Hz, 1H), 7.46 (dd, $J = 2.7$ Hz, 8.8 Hz, 1H), 7.40 (d, $J = 8.7$ Hz, 1H), 7.01 (d, $J = 8.8$ Hz, 1H), 2.34 (s, 3H). LCMS (*m*/*z*): $[M - H^-]^-$ calcd for $[C_{14}H_{11}Cl_2NO_2]$, 294.01; found, 294.19.

***N*-(4-Trifluoromethylsulfanylphenyl)-2-acetoxy-5-iodobenzamide (28a).** ^{1}H NMR ($CDCl_3$): δ 8.31 (s, 1H), 8.04 (d, $J = 2.2$ Hz, 1H), 7.77 (dd, $J = 8.5$ Hz, 6.3 Hz, 1H), 7−59-7.64 (m, 4H), 6.89 (d, $J = 8.53$ Hz, 1H), 2.31 (s, 3H). LCMS (*m*/*z*): $[M - H^-]^-$ calcd for $[C_{16}H_{11}F_3INO_3S]$, 479.94; found $[-Ac^+]$, 438.11.

***N*-(4-Trifluoromethylsulfanylphenyl)-2-hydroxy-5-iodobenzamide (28b).** ^{1}H NMR (MeOD): δ 8.28 (s, 1H), 7.84 (d, J = 8.5 Hz, 2H), 7.75−7.64 (m, 3H), 6.80 (d, J = 8.7 Hz, 1H). LCMS (*m*/*z*): $[M - H^-]^-$ calcd for $[C_{14}H_9F_3INO_2S]$, 437.93; found, 437.96.

***N*-(4-Bromophenyl)-2-acetoxy-3-chlorobenzamide (29a).** ^{1}H NMR (DMSO): δ 10.57 (s, 1H), 7.76 (dd, J = 8.1 Hz, 6.6 Hz, 1H), 7.70−7.63 (m, 3H), 7.56−7.52 (m, 2H), 7.45 (t, J = 7.9 Hz, 1H), 2.26 (s, 3H). LCMS (*m*/*z*): $[M - H^-]^-$ calcd for $[C_{15}H_{11}BrClNO_3]$, 365.95; found $[-Ac^+]$, 324.07.

***N*-(4-Bromophenyl)-3-chloro-2-hydroxybenzamide (29b).** ^{1}H NMR (MeOD): δ 7.88 (d, J = 7.8 Hz, 1H), 7.64 (d, J = 8.8 Hz, 2H), 7.56 (d, J = 8.3 Hz, 1H), 7.52 (d, J = 8.8 Hz, 2H), 6.96−6.89 (m, 1H). LCMS (*m*/*z*): $[M - H^-]^-$ calcd for $[C_{13}H_9BrClNO_2]$, 323.94; found, 324.00.

Acknowledgment. We thank the Swedish National Research Council, the Swedish Governmental Agency for Innovation Systems (VINNOVA), the Foundation for Technology Transfer in Umeå, the Carl Trygger foundation, Innate Pharmaceuticals, and Umeå Biotech Incubator for support.

Supporting Information Available: Information on BBs, descriptors, and other variable selection criteria are given. A table of compound purities, LC chromatograms for key compounds, and ^{1}H NMR spectra of all compounds are also given. This material is available free of charge via the Internet at http://pubs.acs.org.

References

(1) Levy, S. B. Antibiotic resistance—the problem intensifies. *Adv. Drug Delivery Rev.* **2005**, *57*, 1446−1450.
(2) Poole, K. Multidrug resistance in Gram-negative bacteria. *Curr. Opin. Microbiol.* **2001**, *4*, 500−508.
(3) Normark, S.; Nilsson, C.; Normark, B. H. Microbiology—A pathogen attacks while keeping up defense. *Science* **2005**, *307*, 1211−1212.
(4) Brundtland, G. H. *Overcoming antimicrobial resistance*. World Health Report on Infectious Diseases; Geneva, Switzerland, 2000.
(5) Henry, C. M. Antibiotic resistance. *Chem. Eng. News* **2000**, *78*, 41−58.
(6) Hawley, R. J.; Eitzen, E. M. Biological weapons—A primer for microbiologists. *Annu. Rev. Microbiol.* **2001**, *55*, 235−253.
(7) Inglesby, T. V.; Dennis, D. T.; Henderson, D. A.; Bartlett, J. G.; Ascher, M. S.; Eitzen, E.; Fine, A. D.; Friedlander, A. M.; Hauer, J.; Koerner, J. F.; Layton, M.; McDade, J.; Osterholm, M. T.; O'Toole, T.; Parker, G.; Perl, T. M.; Russell, P. K.; Schoch-Spana, M.; Tonat, K. Plague as a biological weapon—Medical and public health management. *JAMA, J. Am. Med. Assoc.* **2000**, *283*, 2281−2290.
(8) Goldschmidt, R. M.; Macielag, M. J.; Hlasta, D. J.; Barrett, J. F. Inhibition of virulence factors in bacteria. *Curr. Pharm. Des.* **1997**, *3*, 125−142.
(9) Lee, Y. M.; Almqvist, F.; Hultgren, S. J. Targeting virulence for antimicrobial chemotherapy. *Curr. Opin. Pharmacol.* **2003**, *3*, 513−519.
(10) Walsh, C. Where will new antibiotics come from? *Nat. Rev. Microbiol.* **2003**, *1*, 65−70.
(11) Hueck, C. J. Type III protein secretion systems in bacterial pathogens of animals and plants. *Microbiol. Mol. Biol. Rev.* **1998**, *62*, 379−433.
(12) Perry, R. D.; Fetherston, J. D. *Yersinia pestis*—Etiologic agent of plague. *Clin. Microbiol. Rev.* **1997**, *10*, 35−66.
(13) Wren, B. W. The Yersiniae—A model genus to study the rapid evolution of bacterial pathogens. *Nat. Rev. Microbiol.* **2003**, *1*, 55−64.
(14) Cornelis, G. R. Molecular and cell biology aspects of plague. *Proc. Natl. Acad. Sci. U.S.A.* **2000**, *97*, 8778−8783.
(15) Cornelis, G. R.; WolfWatz, H. The Yersinia Yop virulon: A bacterial system for subverting eukaryotic cells. *Mol. Microbiol.* **1997**, *23*, 861−867.
(16) Muller, S.; Feldman, M. F.; Cornelis, G. R. The type III secretion system of Gram-negative bacteria: A potential therapeutic target? *Expert Opin. Ther. Targets* **2001**, *5*, 327−339.
(17) Gauthier, A.; Finlay, B. B. Type III secretion system inhibitors are potential antimicrobials—Present in disease-causing Gram-negative bacteria, components of this system might be good targets for novel antimicrobial agents. *ASM News* **2002**, *68*, 383−387.
(18) Bailey, L.; Gylfe, A.; Sundin, C.; Muschiol, S.; Elofsson, M.; Nordstrom, P.; Henriques-Normark, B.; Lugert, R.; Waldenstrom, A.; Wolf-Watz, H.; Bergstrom, S. Small molecule inhibitors of type III secretion in *Yersinia* block the *Chlamydia pneumoniae* infection cycle. *FEBS Lett.* **2007**, *581*, 587−595.
(19) Kauppi, A. M.; Nordfelth, R.; Uvell, H.; Wolf-Watz, H.; Elofsson, M. Targeting bacterial virulence: Inhibitors of type III secretion in *Yersinia*. *Chem. Biol.* **2003**, *10*, 241−249.
(20) Muschiol, S.; Bailey, L.; Gylfe, A.; Sundin, C.; Hultenby, K.; Bergstrom, S.; Elofsson, M.; Wolf-Watz, H.; Normark, S.; Henriques-Normark, B. A small-molecule inhibitor of type III secretion inhibits different stages of the infectious cycle of *Chlamydia trachomatis*. *Proc. Natl. Acad. Sci. U.S.A.* **2006**, *103*, 14566−14571.
(21) Nordfelth, R.; Kauppi, A. M.; Norberg, H. A.; Wolf-Watz, H.; Elofsson, M. Small-molecule inhibitors specifically targeting type III secretion. *Infect. Immun.* **2005**, *73*, 3104−3114.
(22) Wolf, K.; Betts, H. J.; Chellas-Gery, B.; Hower, S.; Linton, C. N.; Fields, K. A. Treatment of *Chlamydia trachomatis* with a small molecule inhibitor of the *Yersinia* type III secretion system disrupts progression of the chlamydial developmental cycle. *Mol. Microbiol.* **2006**, *61*, 1543−1555.
(23) Bailey, L.; Gylfe, A.; Sundin, C.; Muschiol, S.; Elofsson, M.; Nordstrom, P.; Henriques-Normark, B.; Lugert, R.; Waldenstrom, A.; Wolf-Watz, H.; Bergstrom, S. Small molecule inhibitors of type III secretion in *Yersinia* block the *Chlamydia pneumoniae* infection cycle. *FEBS Lett.* **2007**, *581*, 587−595.
(24) Gauthier, A.; Robertson, M. L.; Lowden, M.; Ibarra, J. A.; Puente, J. L.; Finlay, B. B. Transcriptional inhibitor of virulence factors in enteropathogenic *Escherichia coli*. *Antimicrob. Agents Chemother.* **2005**, *49*, 4101−4109.
(25) Kauppi, A. M.; Nordfelth, R.; Hagglund, U.; Wolf-Watz, H.; Elofsson, M. Salicylanilides are potent inhibitors of type III secretion in *Yersinia*. *Adv. Exp. Med. Biol.* **2003**, *529*, 97−100.
(26) Lee, V. T.; Pukatzki, S.; Sato, H.; Kikawada, E.; Kazimirova, A. A.; Huang, J.; Li, X. H.; Arm, J. P.; Frank, D. W.; Lory, S. Pseudolipasin A is a specific inhibitor for phospholipase A(2) activity of *Pseudomonas aeruginosa* cytotoxin ExoU. *Infect. Immun.* **2007**, *75*, 1089−1098.
(27) Tautz, L.; Bruckner, S.; Sareth, S.; Alonso, A.; Bogetz, J.; Bottini, N.; Pellecchia, M.; Mustelin, T. Inhibition of *Yersinia* tyrosine phosphatase by furanyl salicylate compounds. *J. Biol. Chem.* **2005**, *280*, 9400−9408.
(28) Alksne, L. E.; Projan, S. J. Bacterial virulence as a target for antimicrobial chemotherapy. *Curr. Opin. Biotechnol.* **2000**, *11*, 625−636.
(29) Marra, A. Targeting virulence for antibacterial chemotherapy-identifying and characterizing virulence factors for lead discovery. *Drugs R&D* **2006**, *7*, 1−16.
(30) Becker, D.; Selbach, M.; Rollenhagen, C.; Ballmaier, M.; Meyer, T. F.; Mann, M.; Bumann, D. Robust *Salmonella* metabolism limits possibilities for new antimicrobials. *Nature* **2006**, *440*, 303−307.
(31) Burbaum, J. J.; Sigal, N. H. New technologies for high-throughput screening. *Curr. Opin. Chem. Biol.* **1997**, *1*, 72−78.
(32) Hung, D. T.; Shakhnovich, E. A.; Pierson, E.; Mekalanos, J. J. Small-molecule inhibitor of *Vibrio cholerae* virulence and intestinal colonization. *Science* **2005**, *310*, 670−674.
(33) Jorgensen, W. L. The many roles of computation in drug discovery. *Science* **2004**, *303*, 1813−1818.
(34) Linusson, A.; Gottfries, J.; Lindgren, F.; Wold, S. Statistical molecular design of building blocks for combinatorial chemistry. *J. Med. Chem.* **2000**, *43*, 1320−1328.
(35) Linusson, A.; Gottfries, J.; Olsson, T.; Örnskov, E.; Folestad, S.; Norden, B.; Wold, S. Statistical molecular design, parallel synthesis, and biological evaluation of a library of thrombin inhibitors. *J. Med. Chem.* **2001**, *44*, 3424−3439.
(36) Martin, E. J.; Blaney, J. M.; Siani, M. A.; Spellmeyer, D. C.; Wong, A. K.; Moos, W. H. Measuring diversity—Experimental-design of combinatorial libraries for drug discovery. *J. Med. Chem.* **1995**, *38*, 1431−1436.
(37) Hansch, C. A quantitative approach to biochemical structure−activity relationships. *Acc. Chem. Res.* **1969**, *2*, 232−239.
(38) Wold, S.; Dunn, W. J., III. Multivariate quantitative structure−activity relationships (QSAR): Conditions for their applicability. *J. Chem. Inf. Model.* **1983**, *23*, 6−13.
(39) Eriksson, L.; Johansson, E. Multivariate design and modeling in QSAR. *Chemom. Intell. Lab. Syst.* **1996**, *34*, 1−19.
(40) Larsson, A.; Johansson, S.; Pinkner, J. S.; Hultgren, S. J.; Almqvist, F.; Kihlberg, J.; Linusson, A. Multivariate design, synthesis, and biological evaluation of of peptide inhibitors of FimC/FimH protein−protein interactions in uropathogenic *Escherichia coli*. *J. Med. Chem.* **2005**, *48*, 935−945.

(41) Wold, S.; Josefson, M.; Gottfries, J.; Linusson, A. The utility of multivariate design in PLS modeling. *J. Chemom.* **2004**, *18*, 156−165.
(42) Wold, S.; Ruhe, A.; Wold, H.; Dunn, W. J. The collinearity problem in linear regression. The partial least squares approach to generalized inverses. *SIAM J. Sci. Stat. Comput.* **1984**, *5*, 735−743.
(43) Wold, S.; Sjostrom, M.; Eriksson, L. PLS-regression: a basic tool of chemometrics. *Chemom. Intell. Lab. Syst.* **2001**, *58*, 109−130.
(44) Wold, S.; Esbensen, K.; Geladi, P. Principal component analysis. *Chemom. Intell. Lab. Syst.* **1987**, *2*, 37−52.
(45) Eriksson, L.; Johansson, E.; Lindgren, F.; Sjöstrom, M.; Wold, S. Megavariate analysis of hierarchical QSAR data. *J. Comput.-Aided Mol. Des.* **2002**, *16*, 711−726.
(46) Olsson, I. M.; Gottfries, J.; Wold, S. D-optimal onion designs in statistical molecular design. *Chemom. Intell. Lab. Syst.* **2004**, *73*, 37−46.
(47) deAguiar, P. F.; Bourguignon, B.; Khots, M. S.; Massart, D. L.; PhanThanLuu, R. D-optimal designs. *Chemom. Intell. Lab. Syst.* **1995**, *30*, 199−210.
(48) Johnson, M. E.; Nachtseim, C. J. Some guidelines for constructing exact D-optimal designs on convex spaces. *Technometrics* **1983**, *25*, 271−277.
(49) Sjöström, M.; Wold, S.; Söderström, B. *PLS discriminant plots*. Proceedings of PARC in Practice, Amsterdam, The Netherlands, June 19−21, 1985; Elsevier Science Publ. B. V.: North Holland, 1986; pp 461−470.
(50) Terada, H.; Goto, S.; Yamamoto, K.; Takeuchi, I.; Hamada, Y.; Miyake, K. Structural requirements of salicylanilides for uncoupling activity in mitochondria−Quantitative-analysis of structure−uncoupling relationships. *Biochim. Biophys. Acta* **1988**, *936*, 504−512.
(51) Macielag, M. J.; Demers, J. P.; Fraga-Spano, S. A.; Hlasta, D. J.; Johnson, S. G.; Kanojia, R. M.; Russel, R. K.; Sui, Z. H.; Weidner-Wells, M. A.; Werblood, H.; Foleno, B. D.; Goldschmidt, R. M.; Loeloff, M. J.; Webb, G. C.; Barrett, J. F. Substituted salicylanilides as inhibitors of two-component regulatory systems in bacteria. *J. Med. Chem.* **1998**, *41*, 2939−2945.
(52) Stephenson, K.; Yamaguchi, Y.; Hoch, J. A. The mechanism of action of inhibitors of bacterial two-component signal transduction systems. *J. Biol. Chem.* **2000**, *275*, 38900−38904.
(53) Kim, C.C.; Falkow, S. Delineation of upstream signaling events in the salmonella pathogenicity island 2 transcriptional activation pathway. *J. Bacteriol.* **2004**, *186*, 4694−4704.
(54) Xiao, Y. M.; Lan, L. F.; Yin, C. T.; Deng, X.; Baker, D.; Zhou, J. M.; Tang, X. Y. Two-component sensor RhpS promotes induction of Pseudomonas syringae type III secretion system by repressing negative regulator RhpR. *Mol. Plant-Microbe Interact.* **2007**, *20*, 223−234.
(55) Barrett, J. F.; Isaacson, R. E. *Annual Reports in Medicinal Chemistry*; Academic Press: San Diego, CA, 1995; pp 111−118.
(56) Payne, D. J.; Gwynn, M. N.; Holmes, D. J.; Pompliano, D. L. Drugs for bad bugs: confronting the challenges of antibacterial discovery. *Nat. Rev. Drug Discovery* **2007**, *6*, 29−40.
(57) *ChemACX2002*; CambridgeSoft: Cambridge, MA, 2002.
(58) *MOE*. Chemical Computing Group Inc.: Montreal, Quebec, Canada, 2004.
(59) *Umetrics*. *SIMCA-P+* SIMCA-P+ 10.0, 10.5, 11.0; Box 7960, S-907 19 Umeå, Sweden.
(60) Forsberg, A.; Rosqvist, R. In-vivo expression of virulence genes of *Yersinia-pseudotuberculosis*. *Infect Agents Dis.* **1993**, *2*, 275−278.

JM070741B